Neutron powder diffraction study on the iron-based nitride superconductor ThFeAsN

2017 EPL 117 57005

(http://iopscience.iop.org/0295-5075/117/5/57005)

A Letters Journal Exploring the Frontiers of Physics

March 2017

EPL, **117** (2017) 57005 www.epljournal.org
doi: 10.1209/0295-5075/117/57005

Neutron powder diffraction study on the iron-based nitride superconductor ThFeAsN

Huican Mao[1,2], Cao Wang[3], Helen E. Maynard-Casely[4], Qingzhen Huang[5], Zhicheng Wang[6], Guanghan Cao[6,7], Shiliang Li[1,2,8] and Huiqian Luo[1(a)]

[1] *Beijing National Laboratory for Condensed Matter Physics, Institute of Physics, Chinese Academy of Sciences Beijing 100190, China*
[2] *University of Chinese Academy of Sciences - Beijing 100049, China*
[3] *Department of Physics, Shandong University of Technology - Zibo 255049, China*
[4] *Australian Centre for Neutron Scattering, Australian Nuclear Science and Technology Organisation Lucas Heights NSW-2232, Australia*
[5] *NIST Center for Neutron Research, National Institute of Standards and Technology Gaithersburg, MD 20899-6102, USA*
[6] *Department of Physics and State Key Lab of Silicon Materials, Zhejiang University - Hangzhou 310027, China*
[7] *Collaborative Innovation Centre of Advanced Microstructures - Nanjing 210093, China*
[8] *Collaborative Innovation Center of Quantum Matter - Beijing 100190, China*

received 14 March 2017; accepted in final form 7 April 2017
published online 8 May 2017

PACS 74.70.Xa – Superconducting materials other than cuprates: Pnictides and chalcogenides
PACS 74.62.Bf – Superconductivity: Effects of material synthesis, crystal structure, and chemical composition
PACS 74.25.F- – Transport properties

Abstract – We report neutron diffraction and transport results on the newly discovered superconducting nitride ThFeAsN with $T_c = 30\,\mathrm{K}$. No magnetic transition, but a weak structural distortion around 160 K, is observed by cooling from 300 K to 6 K. Analysis on the resistivity, Hall transport and crystal structure suggests that this material behaves as an electron optimally doped pnictide superconductor due to extra electrons from nitrogen deficiency or oxygen occupancy at the nitrogen site, which, together with the low arsenic height, may enhance the electron itinerancy and reduce the electron correlations, thus suppressing the static magnetic order.

Introduction. – Unconventional superconductivity in iron pnictides or chalcogenides has been intensively investigated since the ZrCuSiAs-type crystalline $LaFeAsO_{1-x}F_x$ (1111 family) with transition temperature $T_c = 26$ K was discovered in 2008 [1]. Usually, the iron-based superconductivity emerges from the proximity to a three-dimensional antiferromagnetism [2], for example, $LaFeAsO_{1-x}F_x$ [3,4], $BaFe_{2-x}Co_xAs_2$ (122 family) [5], $NaFe_{1-x}Co_xAs$ (111 family) [6], $FeTe_{1-x}Se_x$ (11 family) [7,8] and $Ca_{1-x}La_xFeAs_2$ (112 family) [9,10], etc. In some special cases, the conductivity is very sensitive to the ion deficiency, such as $LaFeAsO_{1-\delta}$ [11], $Li_{1-\delta}FeAs$ [12] and $K_{0.8}Fe_{2-\delta}Se_2$ [13], or the stoichiometric composition is naturally superconducting, such as Sr_2VO_3FeAs (21311 family) [14], $Ca_{10}(Fe_3Pt_8)(Fe_2As_2)_5$ (10-3-8 family) [15], KFe_2As_2 [16], $RbEuFe_4As_4$ (1144 family) [17], FeSe [18], etc. Even so, in most of the above families, spin fluctuations persist and intimately interplay with superconductivity, while in most parent compounds, a magnetic phase transition always occurs beneath the symmetry-breaking structural transition at low temperature except for the FeSe system [19].

Specifically for the 1111 family, superconductivity can be induced among the antiferromagnetically ordered oxide (*e.g.*, LaFeAsO) [1], fluoride (*e.g.*, CaFeAsF) [20,21] and hydride (*e.g.*, $LaFeAsO_{1-x}H_x$) [22,23] under the chemical substitution on any atomic site. Recently, the first nitride iron pnictide superconductor ThFeAsN, containing layers with nominal compositions $[Th_2N_2]$ and $[Fe_2As_2]$(fig. 1(a)), has been discovered, with $T_c = 30\,\mathrm{K}$

(a) E-mail: hqluo@iphy.ac.cn

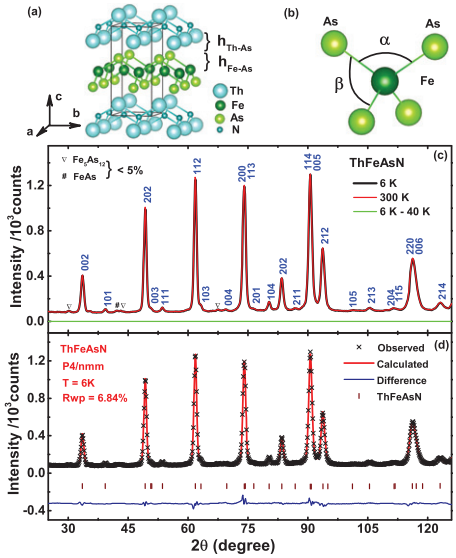

Fig. 1: (Colour online) (a) The crystal structure and (b) $FeAs_4$ tetrahedron of ThFeAsN. $h_{Th\text{-}As}$ and $h_{Fe\text{-}As}$ are arsenic height to Th layer and Fe layer, respectively. α and β indicate the two different As-Fe-As bond angles [24]. (c) Normalized neutron powder diffraction patterns at 6 K and 300 K and the difference between 6 K and 40 K for ThFeAsN. A few peaks of Fe_5As_{12} and FeAs impurity phase are marked. (d) Rietveld refinement results with tetragonal phase $P4/nmm$ space group at 6 K.

for a nominally undoped compound [24]. Although the first-principle calculation of ThFeAsN indicates that the lowest-energy magnetic ground state is the stripe-type antiferromagnetic state [25,26], the normal-state resistivity shows no obvious anomaly but rather a metallic behavior. In principle, the N-N bond covalency may lower the effective nitrogen valence and lead to an internal charge transfer. Such self-doping effect may be responsible for the superconductivity and suppress the magnetic order completely, since any further electron doping via substituting N with O or hole doping via substituting Th with Y only suppress the superconducting T_c [24]. Indeed, the ^{57}Fe Mössbauer spectroscopy study on the polycrystalline samples suggests no magnetically ordered moment on the iron site down to 2 K [27]. To finally clarify the absence of magnetic order and classify the superconductivity with other compounds, neutron powder diffraction experiments are highly desired for this new material.

Experiments. – The polycrystalline samples with T_c = 30 K were synthesized by the solid-state reaction method as described elsewhere [6]. To make homogeneous scattering background sure, 2 grams of powder samples were ground and sealed in a vanadium can. Neutron powder diffraction experiments were carried out on the WOMBAT high-intensity diffractometer at the Australian Centre for Neutron Scattering, Australian Nuclear Science and Technology Organisation. The wavelength of the neutron was selected to be $\lambda = 2.41$ Å. The scattering data was collected at 6 K (4 h), 40 K (4 h) and other temperatures up to 300 K (1 h for each) by covering the scattering angle 2θ range 15–136 degrees. All these diffraction patterns were refined with the Rietveld method within the program FullProf [28], and the temperature dependence of the structure parameters, such as lattice constant, full width at half-maximum (FWHM) of the (112) peak, As-Fe-As bond angles, bond length and the ionic (Th, Fe) height from the As layer, was obtained by assuming 100% occupancy of ThFeAsN. The temperature-dependent resistivity from 2 K to 300 K was measured by the standard 4-probe method, and the Hall coefficient (R_H) was measured by the transverse resistance under sweeping magnetic fields from −6 T to +6 T over the temperature range 50 K–300 K on a *Quantum Design* Physical Property Measurement System (PPMS).

Table 1: Crystallographic data of ThFeAsN at 6 K.

Space group	$P4/nmm$	Rwp (%)	6.84(3)
a (Å)	4.0414(1)	$h_{Th\text{-}As}$(Å)	1.7858(1)
c (Å)	8.5152(1)	$h_{Fe\text{-}As}$(Å)	1.2964(1)
$\alpha_{Fe\text{-}As\text{-}Fe}$	114.65°	$d_{Th\text{-}As}$(Å)	3.3700(3)
$\beta_{Fe\text{-}As\text{-}Fe}$	106.95°	$d_{Fe\text{-}As}$(Å)	2.4010(3)

Atom	Wyckoff	x	y	z	U_{iso}
Th	2c	0.25	0.25	0.1380(3)	0.3768
Fe	2b	0.75	0.25	0.5	0.0934
As	2c	0.25	0.25	0.6522(5)	0.0884
N	2a	0.75	0.25	0	0.7005

Result and discussion. – The raw data of neutron diffraction patterns are presented in fig. 1. To quantitatively compare the neutron diffraction peaks, we have normalized the maximum neutron counts at 300 K to be the same as 6 K and the difference between 6 K and 40 K is obtained by direct subtraction from the raw data after normalization by monitor counts (fig. 1(c)). Most of the reflections can be indexed by a tetragonal phase in a ZrCuSiAs-type structure with the space group $P4/nmm$ ($a = b = 4.0414$ Å, $c = 8.5152$ Å), except for a very small amount of Fe_5As_{12} and FeAs impurity phases (< 5 %), which are not detected in the X-ray diffraction experiment [24,27]. Figure 1(d) shows the Rietveld refinement of the neutron diffraction patterns at 6 K by assuming 100% occupancy of ThFeAsN. The parameters for the quality of this fitting are: profile factor Rp = 6.47(2)%, weighted profile factor Rwp = 6.84(3)%, and reduced χ-square $\chi^2 = 2.93(1)$. All crystallographic parameters listed in table 1 are mostly consistent with previous X-ray diffraction results [24]. Since there is no difference between 6 K and 40 K data sets and all reflections are identified arising from the nuclear structure from 6 K up to 300 K, we thus conclude that there is no magnetic order in ThFeAsN, consistently with the Mössbauer spectroscopy results [27].

We also performed Rietveld refinements with the FullProf program considering other possibilities. The best fitting results are found in three cases: fully occupied compound (ThFeAsN), (2.7 ± 0.8)% N deficiency

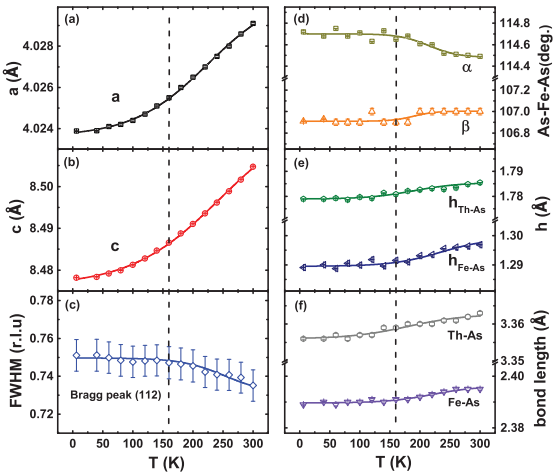

Fig. 2: (Colour online) Temperature dependence of (a) lattice constant a, (b) lattice constant c, (c) FWHM of (112) Bragg peak, (d) As-Fe-As bond angles α and β, (e) anion (Th, Fe) height from the As layer, (f) bond length of Th-As and Fe-As in ThFeAsN.

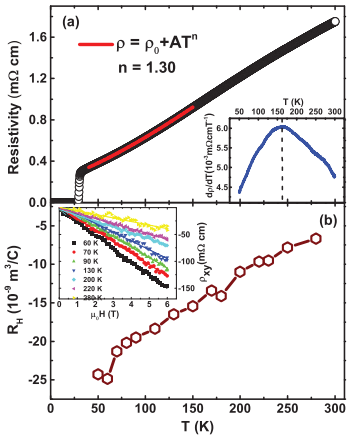

Fig. 3: (Colour online) (a) Temperature dependence of resistivity at zero magnetic field, the inset shows the derivative dR/dT as a function of temperature. (b) Hall coefficient R_H for the ThFeAsN polycrystalline sample, the inset shows the magnetic-field dependence of the Hall resistivity at 60 K, 70 K, 90 K, 130 K, 200 K, 220 K and 280 K.

(ThFeAsN$_{0.97}$) or (7 ± 2)% O occupancy at N site (ThFeAsN$_{0.93}$O$_{0.07}$), among which there is no remarkable difference of the reliability of factors between ThFeAsN. For ThFeAsN$_{0.97}$, the factors are Rp = 6.45(2)%, Rwp = 6.82(2)%, and χ^2 = 2.92(2), and for ThFeAsN$_{0.93}$O$_{0.07}$ they are Rp = 6.45(1)%, Rwp = 6.82(2)%, and χ^2 = 2.93(1). Other cases such as Th or As deficiency give much worse factors, even failure of the fitting. Although the N deficiency or O occupancy as well as the exact proportions of them cannot be distinguished precisely within the data quality and instrument resolution, the N deficiency is more possibly indicated by the refinements due to a larger neutron cross-section of nitrogen.

To search for a possible structural transition in ThFeAsN, we have collected diffraction patterns over the temperature range from 300 K to 6 K. All of them can be well refined with the tetragonal phase of ThFeAsN with the same data as those at room temperature. Therefore, there is no tetragonal-to-orthorhombic transition in lattice. Figure 2 summarizes the temperature dependence of parameters from the Rietveld analysis: the lattice constants (a, c), ionic (Th, Fe) height from the As layer ($h_{Th\text{-}As}$, $h_{Fe\text{-}As}$), the bond angle As-Fe-As (α, β) and the bond length of Fe-As and Th-As. The data sets are nearly unchanged when considering N deficiency or O occupancy. Although the lattice parameters continuously increase with temperature due to thermal expansion, there is a broad kink existing around 160 K for other parameters, a similar feature is also found in the peak width of (112). This can be explained by a weak distortion of the $FeAs_4$ tetrahedron (fig. 1(b)), which may not be strong enough to induce a structural transition similar to some optimally doped iron pnictides [29,30]. Further experiments on the single crystal will be much helpful to clarify this issue.

In order to get an insight into the transport properties at normal state, we have carried out temperature dependence of resistivity and Hall effect measurements on the polycrystalline ThFeAsN, as shown in fig. 3. The resistivity data shows a metallic behavior above T_c without any clear anomaly expected for a magnetic or structural transition. It can be fitted by an empirical power law $\rho = \rho_0 + AT^n$ in a wide temperature range (40 K–150 K) with the exponent n approximate to 1.30, suggesting possible non-Fermi-liquid behaviors governed by quantum fluctuations similar to systems around the optimal doping level [5,31–33]. Interestingly, the derivative dR/dT (insert of fig. 3(a)) also shows a broad hump around 160 K, corresponding to the lattice distortion found in fig. 2. The Hall coefficient (R_H), determined by the slope of the field dependence of the Hall resistivity, is always negative and increases with temperature. By comparing with (La, Sm)FeAsO$_{1-x}$F$_x$ [34,35], the magnitude of R_H in ThFeAsN suggests it is already doped by electrons, which are probably introduced by the N deficiency or O occupancy shown in the powder diffraction refinement, or the reduced valence of nitrogen as discussed before.

By summarizing the literature that has noted the arsenic height $h_{Fe\text{-}As}$, As-Fe-As bond angle α and optimized T_c for each system of iron-based superconductors, it is found that there is a close relationship between the local structure of the $FeAs_4$ tetrahedron and superconducting T_c, as shown by the light blue belt in fig. 4 [36–38]. Obviously, the maximum T_c was achieved when the $FeAs_4$ tetrahedron is perfectly regular, with the bond angle of 109.47 degrees [39]. Interestingly, the data obtained from ThFeAsN agrees very well with other optimally doped compounds (red stars in fig. 4). Again, these results suggest ThFeAsN is nearly in an optimized superconducting state with lots of itinerant electrons and away from the "parent" compound. Another fact should be

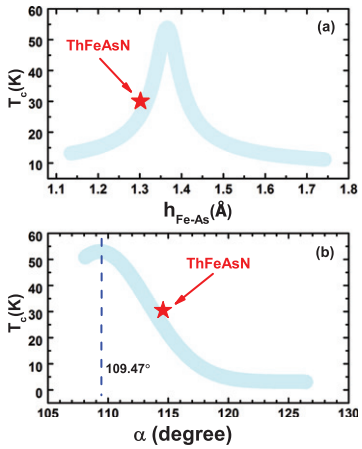

Fig. 4: (Colour online) (a) Anion height dependence of optimal T_c for Fe-based superconductors. (b) Optimal T_c *vs.* bond angle α. The light cyan belts are from other optimally doped systems [38], and the red stars indicate our ThFeAsN compound, respectively.

noticed, *i.e.*, the $h_{Fe\text{-}As}$ of ThFeAsN (1.2964 Å) is lower than those of LaFeAsO (1.3166 Å) [3,4] and SrFeAsF (1.3710 Å) [20,21]. The closer distance of Fe-As will surely favor the electron hopping, thus reducing the electron correlations and orbital order controlled by the Hund coupling J_H within one atomic site [40,41]. This is a reasonable explanation for the absence of magnetic order, structural transition, and resistivity anomaly in ThFeAsN.

Summary. – In summary, we have carried out neutron diffraction experiments on synthesized ThFeAsN over a temperature range from 6 K to 300 K. It is seen that there is neither structural transition nor magnetic transition existing in ThFeAsN, but a structural distortion may occur around 160 K. By comparing with other iron pnictides, we conclude that ThFeAsN may be placed near the optimal doping level and have reduced electron correlations.

* * *

The authors are grateful for the help with the neutron scattering experiment from Dr Guochu Deng at Australian Centre for Neutron Scattering, ANSTO. This work is supported by the National Natural Science Foundation of China (Nos. 11374011, 11374346, 11674406, 11674372 and 11304183), the Strategic Priority Research Program (B) of CAS (XDB07020300), the Ministry of Science and Technology of China (No. 2016YFA0300502) and the Youth Innovation Promotion Association of CAS (No. 2016004). SL and HL acknowledge the project supported by NPL, CAEP (No. 2015AB03).

REFERENCES

[1] Kamihara Y., Watanabe T., Hirano M. and Hosono H., *J. Am. Chem. Soc.*, **130** (2008) 3296.
[2] Dai P. C., *Rev. Mod. Phys.*, **87** (2015) 855.
[3] de la Cruz C. *et al.*, *Nature (London)*, **453** (2008) 899.
[4] Huang Q., Zhao J., Lynn J. W., Chen G. F., Luo J. L., Wang N. L. and Dai P. C., *Phys. Rev. B*, **78** (2008) 054529.
[5] Shibauchi T., Carrington A. and Matsuda Y., *Annu. Rev. Condens. Matter Phys.*, **5** (2014) 113.
[6] Parker D. R. *et al.*, *Phys. Rev. Lett.*, **104** (2010) 057007.
[7] Liu T. J. *et al.*, *Nat. Mater.*, **9** (2010) 716.
[8] Katayama N. *et al.*, *J. Phys. Soc. Jpn.*, **79** (2010) 113702.
[9] Katayama N. *et al.*, *J. Phys. Soc. Jpn.*, **82** (2013) 123702.
[10] Jiang S. *et al.*, *Phys. Rev. B*, **93** (2016) 174513.
[11] Ren Z.-A. *et al.*, *EPL*, **83** (2008) 17002.
[12] Wang X. C., Liu Q. Q., Lv Y. X., Gao W. B., Yang L. X., Yu R. C., Li F. Y. and Jin C. Q., *Solid State Commun.*, **148** (2008) 538.
[13] Guo J. G., Jin S. F., Wang G., Wang S. C., Zhu K. X., Zhou T. T., He M. and Chen X. L., *Phys. Rev. B*, **82** (2010) 180520(R).
[14] Zhu X. Y. *et al.*, *Supercond. Sci. Technol.*, **21** (2008) 105001.
[15] Ni N. *et al.*, *Proc. Natl. Acad. Sci. U.S.A.*, **108** (2011) E1019.
[16] Chen H. *et al.*, *EPL*, **85** (2009) 17006.
[17] Liu Y. *et al.*, *Phys. Rev. B*, **93** (2016) 214503.
[18] Hsu F.-C. *et al.*, *Proc. Natl. Acad. Sci. U.S.A.*, **105** (2008) 14262.
[19] Wang Q. S. *et al.*, *Nat. Commun.*, **7** (2016) 12182.
[20] Matsuishi S., Inoue Y., Nomura T., Yanagi H., Hirano M. and Hosono H., *J. Am. Chem. Soc.*, **130** (2008) 14428.
[21] Zhu X. Y., Han F., Cheng P., Mu G., Shen B. and Wen H.-H., *EPL*, **85** (2009) 17011.
[22] Iimura S. *et al.*, *Nat. Commun.*, **3** (2012) 943.
[23] Hiraishi M. *et al.*, *Nat. Phys.*, **10** (2014) 300.
[24] Wang C. *et al.*, *J. Am. Chem. Soc.*, **138** (2016) 2170.
[25] Wang G. T. and Shi X. B., *EPL*, **113** (2016) 67006.
[26] Singh D. J., *J. Alloys Compd.*, **687** (2016) 786.
[27] Albedah M. A. *et al.*, *J. Alloys Compd.*, **695** (2017) 1128.
[28] Rodriguezcarvajal J., *Physica B*, **192** (1993) 55.
[29] Lu X. Y. *et al.*, *Phys. Rev. Lett.*, **110** (2013) 257001.
[30] Hu D. *et al.*, *Phys. Rev. Lett.*, **114** (2015) 157002.
[31] Onari S. and Kontani H., *Phys. Rev. Lett.*, **103** (2009) 177001.
[32] Kasahara S. *et al.*, *Phys. Rev. B*, **81** (2010) 184519.
[33] Zhang R. *et al.*, *Phys. Rev. B*, **91** (2015) 094506.
[34] Kohama Y. *et al.*, *Phys. Rev. B*, **79** (2009) 144527.
[35] Liu R. H. *et al.*, *Phys. Rev. Lett.*, **101** (2008) 087001.
[36] Mizuguchi Y. *et al.*, *Supercond. Sci. Technol.*, **23** (2010) 054013.
[37] Okabe H., Takeshita N., Horigane K., Muranaka T. and Akimitsu J., *Phys. Rev. B*, **81** (2010) 205119.
[38] Chen X. H., Dai P. C., Feng D. L., Xiang T. and Zhang F. C., *Natl. Sci. Rev.*, **1** (2014) 371.
[39] Shirage P. M. *et al.*, *Physica C*, **469** (2009) 355.
[40] Tam Y.-T., Yao D.-X. and Ku W., *Phys. Rev. Lett.*, **115** (2015) 117001.
[41] Hu D. *et al.*, *Phys. Rev. B*, **94** (2016) 094504.